complexes[13,19] consist of two signals separated by approximately 5 eV. For this assignment, however, there are different opinions.[20,21] Gray and co-workers reinterpreted that the S 2p high binding energy (HBE) signal of plastocyanin resulted from the oxidation of sulfur as a result of bombardment by the X-rays.[22] Larsson proposed the possibility of LMCT transition for the HBE line.[23] Probably, the photoredox behavior of the Cu(II)-S complexes accounts for the decrease of the Cu $2p_{3/2}$ binding energy and for the induction of the S 2p HBE line.

In conclusion, this study clarified the unique structure of the binuclear Cu(II) complex of glutathione, a typical ligand of biological origin. The essential characteristics of the present Cu(II) complex are unique axial sulfur coordination in a distorted square-pyramidal geometry and the presence of two copper sites via a disulfide bridge. The bond distance and direction of the apical S-Cu(II) are 3.22 Å and bent by 22° from the basal plane, respectively. The internuclear dipolar interaction between two Cu(II) ions is negligibly small, though the Cu(II)-Cu(II) distance via the disulfide bridge is 5.21 Å. The magnetic susceptibility and ESR features of the Cu(II) complex also support the result. Our crystallographic and spectroscopic results provide valuable information for biologically significant glutathione-Cu(II) complexes.

(20) (a) Solomon, E. I.; Clendening, P. J.; Gray, H. B.; Grunthaner, F. J. *J. Am. Chem. Soc.* **1975**, *97*, 3878-3879. (b) Wurzbach, J. A.; Grunthaner, P. J.; Dooley, D. M.; Gray, H. B.; Grunthaner, F. J.; Gay, R. R.; Solomon, E. I. *Ibid.* **1977**, *99*, 1257-1258.

(21) Peeling, J.; Haslett, B. G.; Evans, I. M.; Clark, D. T.; Boulter, D. *J. Am. Chem. Soc.* **1977**, *99*, 1025-1028.

(22) Thompson, M.; Whelan, J.; Zemon, D. J.; Bosnich, B.; Solomon, E. I.; Gray, H. B. *J. Am. Chem. Soc.* **1979**, *101*, 2482-2483.

(23) Larsson, S. *J. Am. Chem. Soc.* **1977**, *99*, 7708-7709.

Acknowledgments. Gratitude is due to Professor U. Weser for X-ray PES measurements, Dr. T. Takita for support, Professor H. Tanaka for pertinent advice, and M. Ohara for comments on the manuscript. This study was supported in part by a grant from the Ministry of Education, Science, and Culture, Japan.

Generalized Molecular Orbital Theory. Application to Borane and Diborane

T. E. Taylor and M. B. Hall*

Contribution from the Department of Chemistry, Texas A&M University, College Station, Texas 77843. *Received January 25, 1980*

Abstract: The effect of electron correlation on the electron distribution and bonding of diborane is examined in several basis sets. The generalized molecular orbital method is used to define optimized orbitals for the configuration interaction calculations. The results indicate that at least double-ζ (two functions per atomic orbital) and polarization functions (*d* functions on B and *p* functions on H) are needed to adequately describe the electron density of diborane. Electron correlation shifts electron density away from the hydrogens, both terminal and bridging, and into the interior of the cluster and increases the direct B-B contribution to the bonding. We have also calculated the dissociation energy of diborane ($B_2H_6 \rightarrow 2BH_3$). The experimental value is 35 kcal/mol, while without electron correlation the theoretical value is only about 20 kcal/mol. Thus, electron correlation increases the stability of the cluster by about 15 kcal/mol. Our results suggest that the substantial effect of electron correlation on the bonding of diborane is a general result and will apply to other cluster systems.

There has been considerable interest in the electronic structure of the electron-deficient borane clusters.[1] Because these clusters are electron deficient, there are one or more low-lying nonbonding orbitals which are unoccupied in the single-determinant approximation. We speculated that this might give rise to important near-degenerate correlation effects in these systems. Furthermore, the B-H bond distance for bridging for boron-hydrogen bonds is longer and closer to dissociation than the terminal boron-hydrogen bonds. Therefore, electron correlation might be more important for these bridging bonds than for the terminal ones.

Diborane, the simplest cluster in this series, was chosen for study by the generalized molecular orbital (GMO) technique.[2] This technique is a simple means of obtaining a set of primary orbitals for use in a configuration interaction (CI) calculation. It is particularly well suited for systems with a large number of electrons in the same region of space as one finds in clusters. In addition to the general question of the importance of electron correlation in the bonding of diborane, the value of the dissociation energy of diborane into two borane fragments has been a matter of controversy. The experimental values cluster around 60 kcal/mol from mass spectral studies[3] and around 35 kcal/mol from kinetic measurements.[4] Previous theoretical works[5] suggest that

Table I. Total Energies and Number of Spin Configurations for BH_3 Calculations[a]

	MIN	DZ	DZP
HF	-26.077	-26.376	-26.390
GMO	-26.095 [13]	-26.393 [13]	-26.410 [13]
GMO CI	-26.125 [61]	-26.423 [61]	-26.429 [61]
GMO PL	-26.125 [61]	-26.429 [280]	-26.463 [595]
GMO SD	-26.125 [61]	-26.438 [517]	-26.495 [1942]
GMO SD(Q)[b]	-26.126	-26.440	-26.500

[a] Atomic units (hartrees); number of spin configurations in brackets. [b] Quadruples estimated from Davidson's formula.

(1) (a) Switkes, E.; Epstein, I. R.; Tossell, J. A.; Stevens, R. M.; Lipscomb, W. N. *J. Am. Chem. Soc.* **1970**, *92*, 3837. (b) Epstein, I. R.; Marynick, D. S.; Lipscomb, W. N. *J. Am. Chem. Soc.* **1973**, *95*, 1760. (c) Lipscomb, W. N. "Boron Hydrides"; W. A. Benjamin: New York, 1963. (d) Yamabe, S.; Minato, T.; Fujimoto, H.; Fukui, K. *Theor. Chim. Acta* **1974**, *32*, 187. (e) Kleier, D. A.; Halgren, T. A.; Hall, J. H.; Lipscomb, W. N. *J. Chem. Phys.* **1974**, *61*, 3905. (f) Muetterties, E. L. "Boron Hydride Chemistry"; Academic Press: New York, 1975.

(2) (a) Hall, M. B. *Chem. Phys. Lett.* **1979**, *61*, 467. (b) *Int. J. Quantum Chem.* **1978**, *14*, 613. (c) *Int. J. Quantum Chem. Symp.* **1979**, *13*, 195.

0002-7863/80/1502-6136$01.00/0

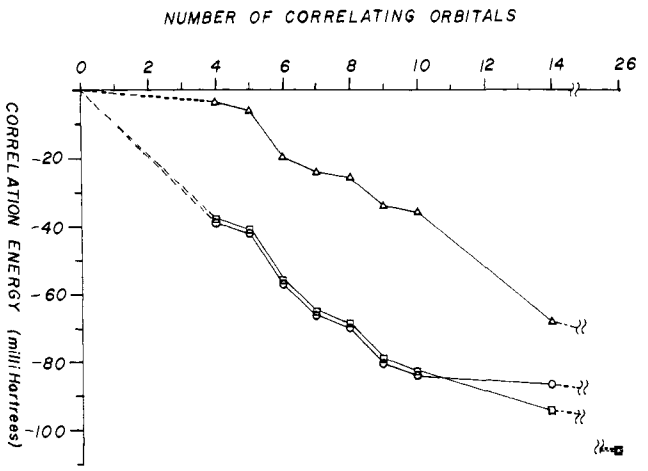

Figure 1. Singles plus doubles correlation energy in the DZP basis as a function of the number of orbitals. Circles represent GMO orbitals, squares represent natural orbitals, and triangles represent Hartree–Fock orbitals. The GMO and HF orbitals were chosen according to their eigenvalues.

Table II. Total Energies and Number of Spin Configurations for B_2H_6 Calculations[a]

	MIN	DZ	DZP
HF	−52.281	−52.771	−52.813
GMO	−52.300 [49]	−52.790 [49]	−52.833 [49]
GMO CI	−52.393 [198]	−52.881 [198]	−52.907 [198]
GMO PL	−52.393 [198]	−52.901 [795]	
GMO SD	−52.393 [198]	−52.914 [1353]	−53.033[b] ± 0.002 [4956]
GMO SD(Q)[c]	−52.399	−52.924	−53.051

[a] Atomic units (hartrees); number of spin configurations in brackets. [b] Extrapolated from A_k threshold calculations. [c] Quadruples estimated from Davidson's formula.

Table III. Calculations of the Dissociation Energy of Diborane[a]

		this work			MBPT[b]	
		MIN	DZ	DZP	TZ	TZP
E_{HF}		9.9	13.3	20.5	13.4	18.5
E_{SD}	GMO CI	10.2	9.5	10.5		
	GMO SD	10.2	10.2	6.7[c]	14.7	16.5
E_Q	GMO CI	2.5	2.5	1.9		
	GMO SD	2.5	4.6	5.8		
E_{ZP}		−5.0	−5.0	−5.0	−5.0	−5.0
E_{RT}		3.9	3.9	3.9	3.9	3.9
E_{DISS}	GMO CI	23.5	24.2	31.8		
	GMO SD	23.5	29.5	31.9	27.0	33.9

[a] kcal mol^{-1}. [b] Reference 6. [c] Estimated from extrapolation of threshold calculations.

a significant fraction of this energy arises from the difference in the electron correlation of B_2H_6 and $2BH_3$.

In this paper we will report calculations on BH_3 and B_2H_6 in several basis sets at various levels of CI. We will also examine the effect of electron correlation on the electron density and the nature of the most important "natural" orbitals. Since Redmon, Purvis, and Bartlett have recently reported a many-body perturbation theory (MBPT) calculation of the dissociation energy,[6] we will place our emphasis on the changes in electron density and orbital structure which are not reported in their MBPT calculations.

Table IV. Total Energies and Number of Configurations in the Threshold Calculations for DZP basis

	total energies[a]		dissociation energy[b]	
	BH_3	B_2H_6	SD	SD(Q)
HF	−26.390	−52.813	20.5	20.5
10^{-3}	−26.439 [96]	−52.870 [96]	−4.9	−5.2
10^{-4}	−26.476 [308]	−52.987 [672]	21.5	25.6
10^{-5}	−26.494 [710]	−53.027 [2643]	24.4	29.8
all SD	−26.495 [1942]	−53.033[c] [4956]	27.2[c]	33.0[c]

[a] Atomic units (hartrees); number of spin configurations in brackets. [b] kcal mol^{-1}; to correct for thermal and vibrational effects, subtract 1.1. [c] Estimated.

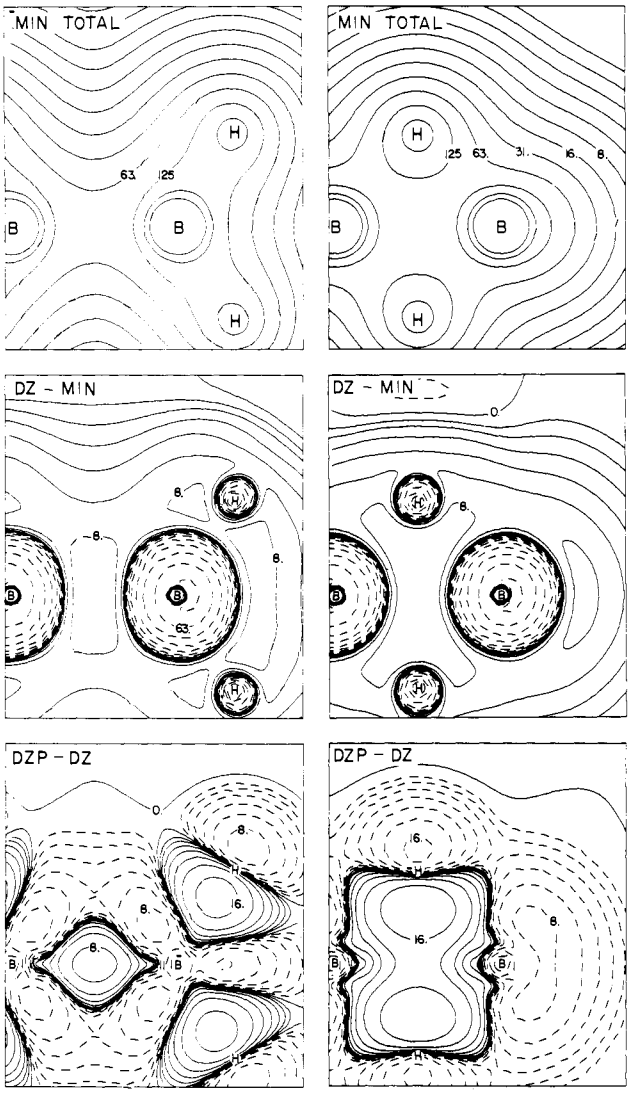

Figure 2. Hartree–Fock electron densities in three basis sets. All plots are 6 by 7 au. Plots in the terminal plane are on the left hand side; the bridging plane plots are on the right. The largest contour marked is 125 millielectrons/au^3. This is $^1/_8$ electron/au^3 or 0.84 electron/Å.^{3} Adjacent contours differ by a factor of 2 in all maps. The first two maps are the Hartree–Fock total electron density of the minimal basis set in two planes. The two center maps represent the difference between the total densities of HF calculations of double-ζ (DZ) and minimal (MIN) basis sets. The last two maps are difference maps of double-ζ plus polarization (DZP) and DZ Hartree–Fock electron densities.

(3) (a) Wilson, J. H.; McGee, H. A. *J. Chem. Phys.* **1967**, *46*, 1444. (b) Ganguli, P. S.; McGee, H. A. *Ibid.* **1969**, *50*, 4658.

(4) (a) Garabedian, M. E.; Benson, S. W. *J. Am. Chem. Soc.* **1964**, *86*, 176. (b) Mappes, G. W.; Fridmann, S. A.; Fehlner, T. P. *J. Phys. Chem.* **1970**, *74*, 3307.

(5) (a) Hall, J. H., Jr.; Marynick, D. S.; Lipscomb, W. N. *Inorg. Chem.* **1972**, *11*, 3126. (b) Edmiston, E.; Lindner, P. *Int. J. Quantum Chem.* **1973**, *7*, 309. (c) Ahlrichs, R. *Theor. Chim. Acta* **1974**, *35*, 59. (d) Marynick, D. S.; Hall, J. H., Jr.; Lipscomb, W. N. *J. Chem. Phys.* **1974**, *61*, 5460.

(6) Redmon, L. T.; Purvis, G. D., III; Bartlett, R. J. *J. Am. Chem. Soc.* **1979**, *101*, 2856.

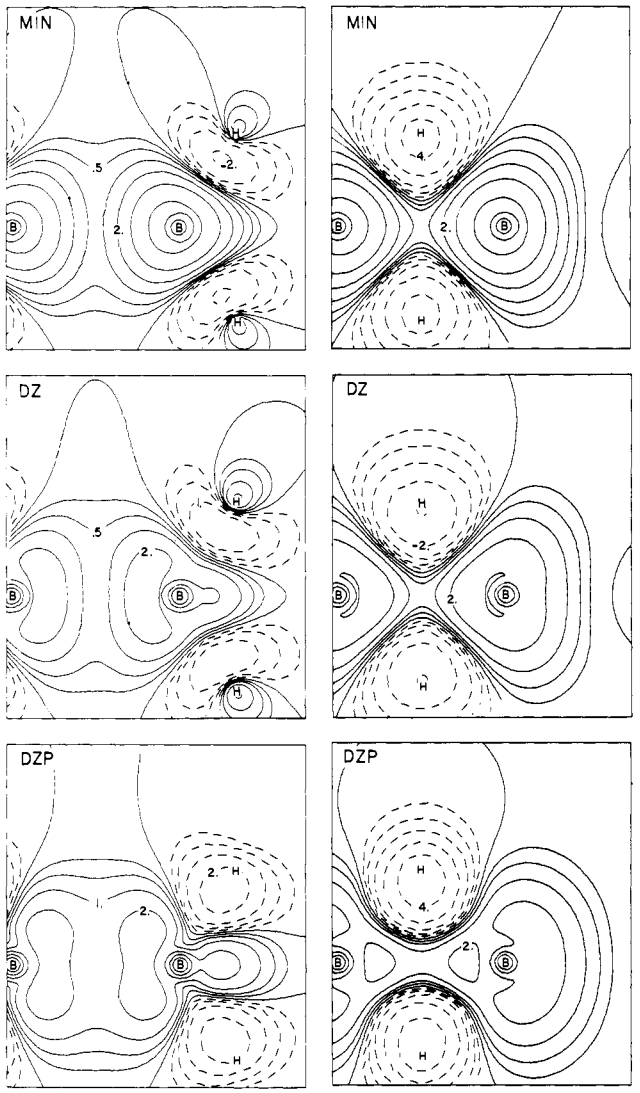

Figure 3. GMO CI minus HF difference maps in three basis sets. Singles plus doubles CI calculations are performed in the GMO framework, involving only 198 configurations from six filled and eight unfilled orbitals. The total electron density from this calculation (GMO CI) is subtracted from the Hartree–Fock electron density.

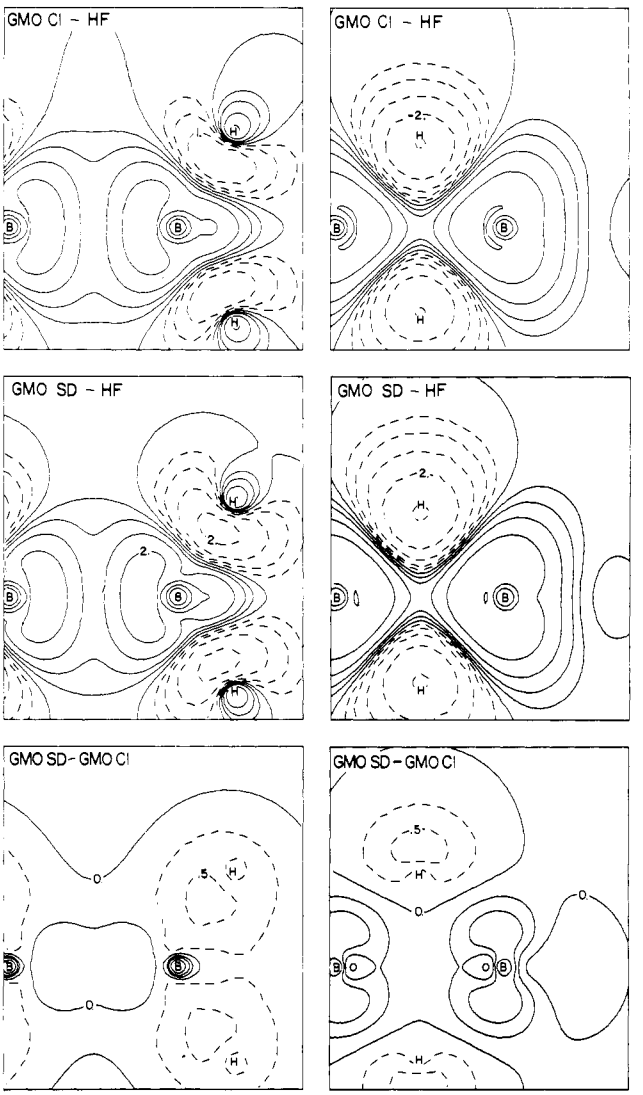

Figure 4. Electron correlation in the double-ζ basis. The difference between the 198 configuration GMO CI electron density and the 1353 configuration all singles plus doubles (GMO SD) is quite small, indicating that our GMO CI level of CI is adequate in describing electron density.

Theory

Generalized Molecular Orbital Theory. The generalized molecular orbital (GMO) approach[2] is a limited type multiconfiguration self-consistent field (MCSCF) calculation which provides an optimized set of primary orbitals for configuration interaction (CI) calculations with only modest additional effort beyond that needed for the Hartree–Fock–Roothaan (HF) or standard molecular orbital (MO) approach. In the standard MO approach for a 2n electron closed-shell molecule, the MO's, which have been expanded in a basis set, are divided into doubly occupied and unoccupied sets as

$$(\phi_1 \cdots \phi_n)^2(\phi_{n+1} \cdots \phi_m)^0 \tag{1}$$

In the GMO approach the previously doubly occupied orbitals are divided into a doubly occupied set (r set) and a strongly occupied set (t set), while the previously unoccupied orbitals are divided into a weakly occupied set (u set) and an unoccupied set (v set). These four sets of orbitals may be thought of as molecular core, valence, valence correlating, and virtual orbitals, respectively. The electronic configuration in the GMO framework may be written as

$$(\phi_1 \cdots)^2(\cdots \phi_n)^x(\phi_{n+1} \cdots)^y(\cdots \phi_m)^0 \tag{2}$$

It is this shell structure, in which the orbitals are treated in groups (sets) with all orbitals in a group (set) having equal occupation numbers, that lead to the use of the name generalized molecular orbital theory.

The GMO wave function, which is consistent with the above orbital partitioning is

$$\psi = (1 - n_t n_u \lambda^2)^{1/2}\psi_{00} + \lambda \sum_t \sum_u \psi_{tu} \tag{3}$$

where

$$\psi_{00} = |\phi_1\bar{\phi}_1 \cdots \phi_t\bar{\phi}_t \cdots \phi_n\bar{\phi}_n| \tag{4}$$

$$\psi_{tu} = |\phi_1\bar{\phi}_1 \cdots \phi_u\bar{\phi}_u \cdots \phi_n\bar{\phi}_n| \tag{5}$$

and n_t and n_u are the number of orbitals in the t and u sets, respectively. Thus, the GMO wave function consists of a dominant single determinant, ψ_{00}, plus a correlation function that contains determinants constructed from all paired excitations from the strongly occupied (t) set to the weakly occupied (u) set. The total energy can be written as in eq 6, where h_i, J_{ij}, and K_{ij} are the

$$E = \sum_i f_i h + \sum_{ij} \sum (a_{ij}J_{ij} + b_{ij}K_{ij}) \tag{6}$$

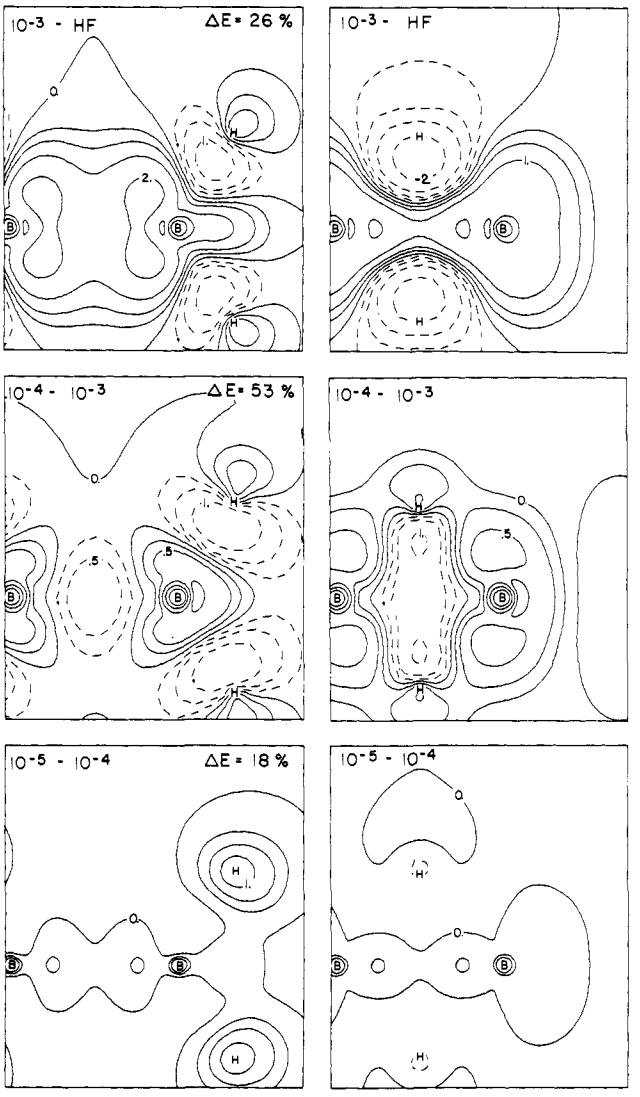

Figure 5. Convergence of electron density in the DZP basis. By using the A_k perturbation method, we select configurations whose estimated contribution to the correlation energy is larger than a given threshold (measured in hartrees). Difference maps between the different threshold calculations indicate that the electron density has essentially converged at the 10^{-4} level, while the energy does not converge until the 10^{-5} level. The ΔE values express the portion of the correlation energy between two different threshold values. Thus, the correlation energies at 10^{-3}, 10^{-4}, and 10^{-5} threshold are 26%, 79%, and 97%, respectively.

one-electron, Coulomb, and exchange integrals, respectively. In standard MO theory $f_t = 2.0$, $a_{ij} = 2.0$, and $b_{ij} = -1.0$. Because these coefficients do not depend on the orbital involved, one can solve the MO problem by the Roothaan procedure.[7] In a general MCSCF problem, these coefficients will depend on the individual orbitals involved. The real advantage of the GMO approach is that these coefficients depend on the set to which the orbitals belong but not on the individual orbitals. Thus, when the variation principle is applied to minimize the energy, the orbitals may be treated in groups as they are in the HF approach. Using a generalized coupling operator[8] to solve this problem, we only need to build two additional HF-like matrices beyond those needed in the ordinary MO approach. Thus, the efforts in obtaining optimized orbitals with the GMO procedure is only a small fraction of that needed by a general MCSCF calculation.

Details of the computational procedure have been given previously.[2] The choice of orbitals for each of the GMO sets is usually straightforward. The strongly occupied set (t) and the weakly occupied set (u) are respectively the filled valence orbitals and the virtual orbitals expected in a minimal basis calculation. Although the filled orbitals from a HF calculation resemble the natural orbitals of extensive CI calculations, the virtual orbitals usually do not bear a similar resemblance. Our previous results for H_2O and N_2 in large Gaussian basis sets showed that the GMO orbitals, both strongly occupied and weakly occupied, resembled the natural orbitals of an all single and double excitation CI calculation. The similarity of the orbitals was reflected both in the overlap between the GMO's and the NO's and in the correlation energies obtained with either set of orbitals.

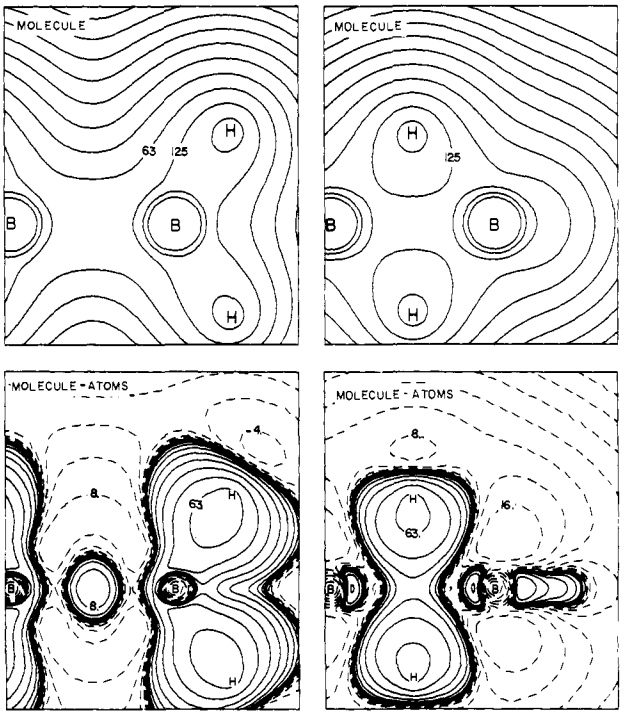

Figure 6. Deformation density map. The first two maps are the total electron density distribution of diborane in the double-ζ plus polarization (DZP) basis and with extended configuration interaction. The density for this calculation should most resemble the experimental electron density of diborane. Subtracting ground-state atomic density from the first two maps yields a theoretical static deformation density map. Our large contours compared favorably with the large contours of the experimental dynamic deformation density maps from X-ray crystallography.

Configuration Interaction. Following the determination of the GMO's, we have done configuration interaction calculations at several levels of accuracy. At the lowest level, we use the orbital space defined by the GMO procedure and perform a CI calculation that involves all possible spin- and symmetry-adapted configurations, which can be constructed from single and double excitations from the t set to the u set. These calculations are referred to as GMO CI. We have also examined polarization CI in the GMO basis (GMO PL), where one electron is allowed into the virtual set (v set), and all valence singles and doubles CI (GMO SD), where two electrons are allowed into the virtual set (v set), except for the core-correlating orbitals. The results of these latter calculations should be similar to an all singles and doubles CI calculation with HF orbitals. We have also compared the GMO orbitals for BH_3 with the natural orbitals of the all singles and doubles calculations.

Because our GMO SD calculation of diborane in our best basis is too large, we have used the A_k perturbation method[9] to select

(7) Roothaan, C. C. J. *Rev. Mod. Phys.* **1951**, *23*, 69.
(8) (a) Hirao, K. *J. Chem. Phys.* **1974**, *60*, 3215. (b) Hirao, K.; Nakatsuji, H. *J. Chem. Phys.* **1973**, *59*, 1457.
(9) Shavitt, I. "Methods of Electronic Structure Theory"; Shafer, H. F., III, Ed.; Plenum Press: New York, **1977**; Chapter 6.

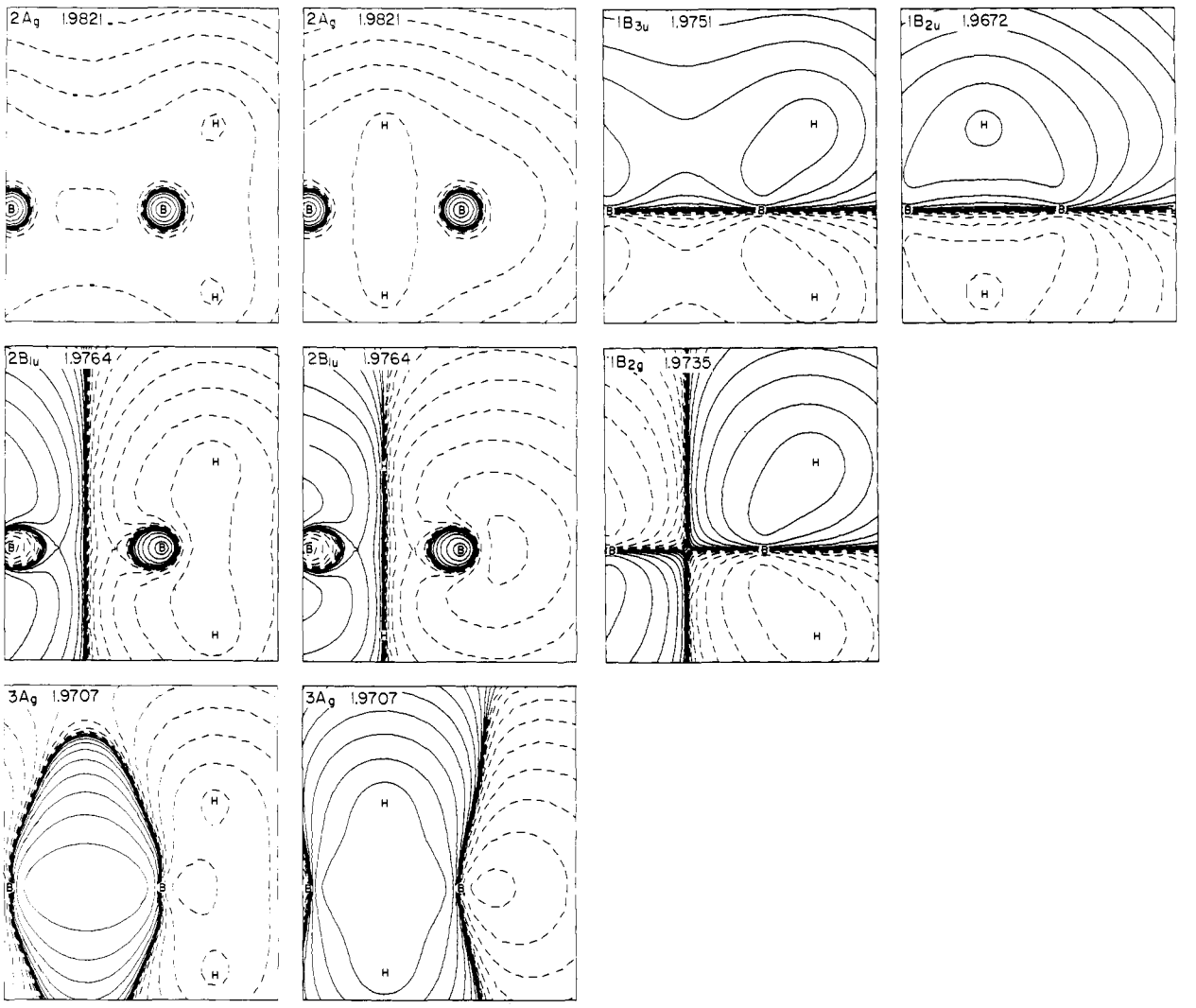

Figure 7. Strongly occupied natural orbitals in the DZP basis. Some planes are not shown because of the nodal properties of symmetry orbitals. Symmetry and occupation numbers are in the upper left hand corner of each map.

smaller subsets of the more important configurations. In the threshold method, all spin configurations contributing less than the specified thresholds to the ground-state function are dropped. We used four thresholds in our best basis: 1×10^{-3}, 1×10^{-4}, 3×10^{-5}, and 1×10^{-5} hartrees. This allows a reliable extrapolation to zero threshold.[10]

One of the next most important contributions to the total energy in a standard CI approach arises from quadruple excitations. In part their importance comes from the fact that the unlinked cluster contributions are neglected in the singles and doubles CI calculation.[9] We have estimated their contribution by using Davidson's formula[11] (eq 7), where ΔE_Q is the energy contribution from

$$\Delta E_Q = \Delta E_D(1 - C_D^2) \quad (7)$$

quadruples and ΔE_D and C_D are the energy contribution and the leading coefficient from the all doubles calculation.

Geometry. The geometry of B_2H_6 was based on the idealized geometry of Lipscomb.[12] Calculations at other geometries[6] show that this geometry is within 1.0 kcal/mol of the optimum one. The geometry of BH_3 was assumed to have D_{3h} symmetry with a B–H bond of 2.25 au. This distance, which was taken from the force field calculations of Gelus and Kutzelnigg,[13] is nearly the same as the terminal B–H distance in B_2H_6.

Basis. Three basis sets were employed in the calculations. The smallest basis set was a minimal Slater basis (MIN) expanded in three Gaussians.[14] The Slater exponents were taken from the optimized ones of Lipscomb[15] (B 1s = 4.68, 2s = 1.4426, 2p = 1.4772, H_b = 1.2095, H_t = 1.1473). For BH_3 we used the same boron exponents and the terminal hydrogen (H_t) exponent. The intermediate basis was Dunning's standard double-ζ contraction (DZ), [4s2p/2s], of Huzinaga's (9s5p/4s) primitive Gaussian basis.[16] The largest basis set employed was formed by adding polarization functions to this intermediate basis. A *d* function with an exponent of 0.70[17] was placed on each boron and a *p* function with an exponent of 1.0[17,18] was placed on each hydrogen.

Calculations. All calculations were carried out on an Amdahl 470 V/6 in double precision at Texas A&M University's Data Processing Center. The integrals and the Hartree–Fock–Roothaan (HF)[7] calculations were done with the ATMOL 2 system of

(10) (a) Buenker, R. J.; Peyerimhoff, S. D. *Theor. Chim. Acta* **1974**, *35*, 33. (b) *Ibid.* **1975**, *39*, 217.
(11) (a) Davidson, E. R. "The World of Quantum Chemistry"; Daudel, R.; Pullman, B., Eds.; Reidel: Dodrecht, Holland, 1974; p 17. (b) Langhoff, S. R.; Davidson, E. R. *Int. J. Quantum Chem.* **1974**, *8*, 61.
(12) Palke, W. E.; Lipscomb, W. N. *J. Chem. Phys.* **1966**, *45*, 3948.
(13) Gelus, M.; Kutzelnigg, W. *Theor. Chim. Acta* **1973**, *28*, 103.
(14) Stewart, R. F. *J. Chem. Phys.* **1970**, *52*, 431.
(15) Switkes, E.; Stevens, R. M.; Lipscomb, W. N. *J. Chem. Phys.* **1969**, *51*, 2085.
(16) (a) Dunning, T. H., Jr. *J. Chem. Phys.* **1970**, *53*, 2823. (b) Huzinaga, S. *Ibid.* **1965**, *42*, 1293.
(17) Dunning, T. H., Jr.; Hay, P. J. "Methods of Electronic Structure Theory"; Schaefer, H. F., III, Ed.; Plenum Press: New York, 1977; Chapter 1.
(18) Dunning, T. H., Jr. *J. Chem. Phys.* **1971**, *55*, 3958.

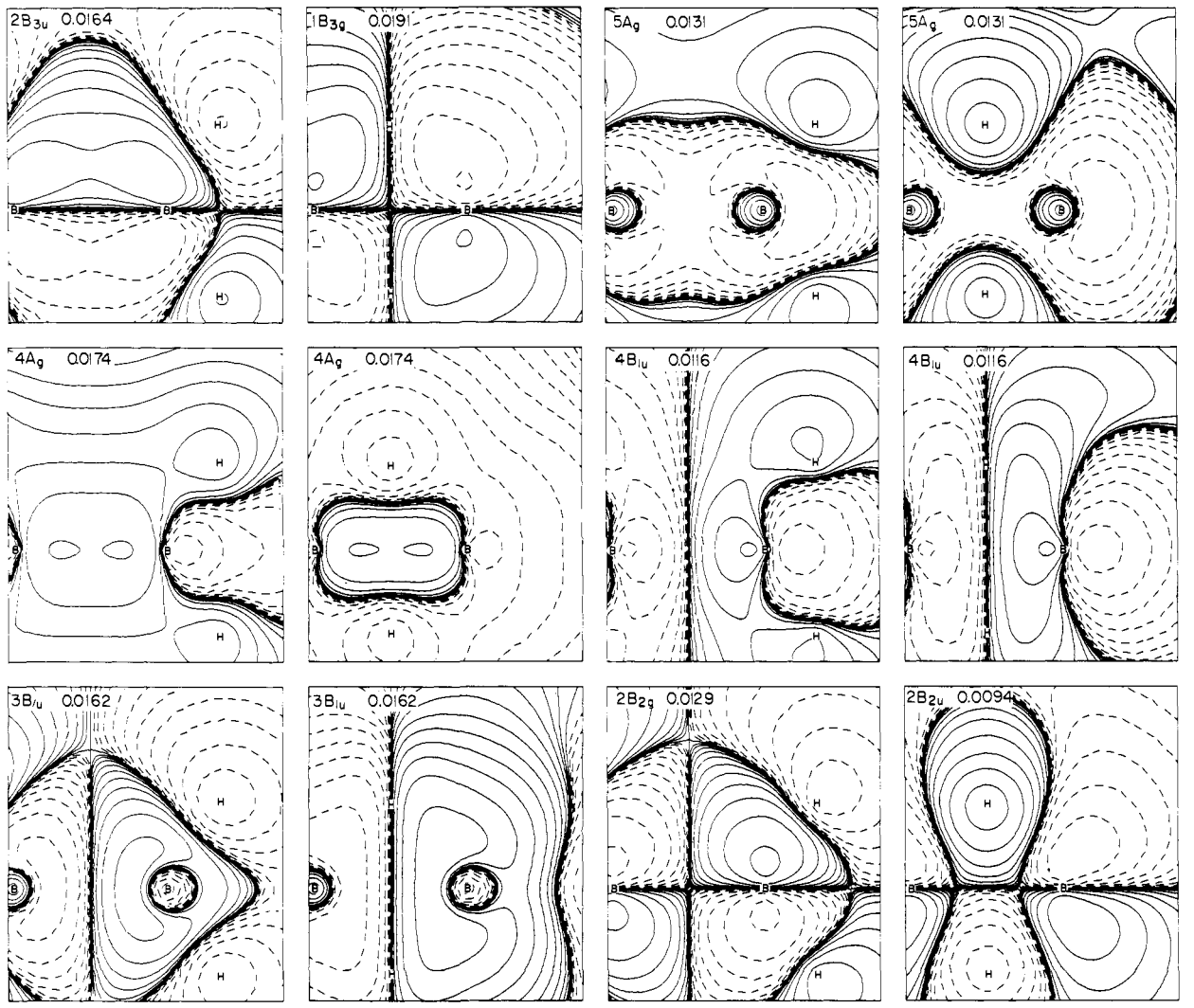

Figure 8. Weakly occupied natural orbitals in the DZP basis.

programs.[19] The GMO calculations were done with a program written by one of the authors (M.B.H.). The CI calculations were done with a package written by Dr. C. T. Corcoran, Dr. J. M. Norbeck, and Professor P. R. Certain. This package, which was written for a Harris computer, was modified by the authors for the Amdahl 470 V/6.

Results and Discussions

Monoborane. Table I gives the total energies and the number of configurations for BH_3 calculations with various basis sets and with various levels of CI. For the GMO calculations on BH_3 the $1a_1'$ orbital was kept doubly occupied (r set), the $2a_1'$ and $1e'$ were the strongly occupied valence (t set) and the $1a_2''$, $2e'$, and $3a'$ were the weakly occupied valence correlating orbitals (u set). As expected the GMO function itself recovers only a small fraction of the correlation energy. However, using the GMO orbitals in a small CI (GMO CI), we recover a substantial portion of the correlation energy of the all singles and doubles calculation with only a small fraction of the configurations. Following the GMO SD calculation, we obtained the natural orbitals (NO) of this wave function by diagonalizing the one-electron density matrix. The most important natural orbitals are nearly identical with the GMO orbitals. Interestingly, the lowest energy GMO virtual orbitals (v set) which are not optimized to correlate the filled ones are also similar to the next most important natural orbitals. This behavior was also seen in calculations on H_2O and N_2.[2c] The rate of convergence with different virtual orbitals toward the all singles and doubles result is shown in Figure 1. One observes that for the most important orbitals the GMO and NO results parallel each other while the results for the HF orbitals are inferior. As one includes additional virtual GMO's, the results begin to diverge from the NO results. Thus, while the GMO's in the u set, which have been optimized to correlate the valence set, and the most important GMO's in the virtual set are very similar to the NO's, the higher energy GMO's do not correspond to the NO's. Thus, the GMO procedure seems to be able to optimize the primary orbitals and provide a reasonable guess at the next most important orbitals.

Diborane. Table II shows the total energy and the number of configurations for B_2H_6 in the three basis and at several levels of CI. Again, we find that the GMO CI results provide a substantial fraction of the correlation energy of the GMO SD calculation with only a fraction of the configurations. For the largest basis a full single and double CI calculation would be too time consuming, so we have estimated this total energy by an extrapolation from the A_k threshold technique.

Dissociation Energy. Table III gives contributions to the predicted dissociation energy according to the partitioning of the energy shown in eq 8, where E_{DISS} is the predicted dissociation

$$E_{DISS} = E_{HF} + E_{SD} + E_Q + E_{ZP} + E_{RT} \qquad (8)$$

energy, E_{HF} is the single-determinant dissociation energy, E_{SD} is the contribution of the singles and doubles CI, E_Q is the estimate of the quadruples contribution, correction. is the zero-point energy,[6] and E_{RT} is the room-temperature correction. These results are

(19) Hillier, I. H.; Saunders, V. R. ATMOL 2 System; Chemistry Department, University of Manchester: Manchester, England.

compared to the recently reported MBPT results.[6] As expected, the values for the minimal and double-ζ basis are too low. However, the value for the double-ζ plus polarization basis is within 3 kcal/mol of the most recent experimental result and the best MBPT result. Our best theoretical estimate is 32 ± 5 kcal/mol^{-1} for reaction (9).

$$B_2H_6 \rightarrow 2BH_3 \quad (9)$$

This value was obtained from extrapolated A_k estimates which are shown in Table IV. The total energies converge fairly rapidly, but slower convergence is observed for the dissociation energy. As the threshold is decreased, the energy of the smaller molecule, BH_3, converges faster than that of the larger molecule, B_2H_6, resulting in a systematic underestimation of the dissociation energy.

Electron Density. We have analyzed the effect of changes in the basis set and the effect of electron correlation by comparing the electron density maps for B_2H_6. Figure 2 shows the results at the HF level. At the top of the figure we have plotted the total electron density for the minimal basis in both the terminal H plane and the bridging H plane. In the center of Figure 2 the electron density difference between the DZ and MIN bases is shown. The large differences near the nuclei are due to the fact that the cusps at the nuclei are poorly represented by the expansion in three Gaussians. In the bonding region we find an increase in electron density in going from the MIN to the DZ bases. At the bottom of the figure the difference between the DZP and DZ bases is shown. Although the energy difference between the DZP and DZ bases is smaller than that between the DZ and MIN bases, the changes in the electron density in the bonding region are of the same magnitude. The addition of polarization functions increases the electron density in the B–H bond region and in the direct B–B bond region. The effects of the 2p orbitals on H are clearly evident. Overall, there is considerable shift of electron density from the outer region of the molecule toward the interior.

Figure 3 shows the effect of electron correlation on the density for all three basis sets. These maps are generated by subtracting the HF electron density from the GMO CI electron density. Although the MIN basis appears to overemphasize the effect of electron correlation, all three sets of maps show similar behavior in the electron density when correlation is introduced. There is considerable movement of electron density away from the bridging hydrogen and from the terminal B–H bond and into the B–B region and the B "lone-pair" region. The overall movement of charge is away from the areas where there are bonds into the previously nonbonding areas. Thus, in the terminal H plane there is movement of electron density toward the B–B region, while in the bridging H plane there is movement of electron density to the "lone-pair" region at the terminal end of the boron.

In order to assess the accuracy of the GMO CI wave function discussed in the previous paragraph, we have examined the electron density changes for the GMO CI and all single and double CI (GMO SD) in the double-ζ basis. These results are shown in Figure 4. At the top we have the difference between the GMO CI and the HF results, while in the center we have the difference between the GMO SD and the HF results. In a qualitative sense these two maps are quite similar and their difference, shown at the bottom of Figure 4, suggests that they are quantitatively very similar. Thus, the GMO CI procedure not only provides a substantial fraction of the correlation energy and a reasonably good value for the dissociation energy of B_2H_6, but it also contains the major changes in the electron density. This is also true of the DZP basis even though GMO CI in this basis yields a smaller fraction of the GMO SD correlation energy.

The difference in electron density as a function of the threshold levels of 10^{-3}, 10^{-4}, and 10^{-5} hartrees is illustrated in Figure 5. The electron density appears to converge more rapidly than the energy, except for a small region around the terminal hydrogens.

Deformation Density. The electron density from our best calculation is shown in Figure 6. By subtracting ground-state atomic densities in the same basis set, we can obtain the static deformation density, which is shown at the bottom of Figure 6. This deformation density shows those changes in the electron density which occur on forming the molecule from its constituent atoms. The largest contours in the deformation density correspond to a buildup of density along the lines connecting the borons and hydrogens. These features are also present in the experimental deformation density.[20] There are two somewhat smaller features which are apparent in the theoretical maps but are too small to be seen in the experimental maps that have been reported to date. The first is a loss of electron density behind the hydrogen atoms, and the second is a buildup of density directly between the borons. This latter feature is also missing in theoretical density maps with minimal basis sets which show a loss of density directly between the borons.[21]

Natural Orbitals. The strongly occupied natural orbitals of our best CI in the DZP basis are shown in Figure 7, while the important weakly occupied natural orbitals are shown in Figure 8. For those orbitals which are zero in one plane only the nonzero plane is shown. The $2a_g$ and $2b_{1u}$ primarily involve the B 2s and H 1s. The $2a_g$ is B–B and B–H bonding while the $2b_{1u}$ is B–B antibonding, B–H_b nonbonding, and B–H_t bonding. The next four strongly occupied orbitals $3a_g$, $1b_{3u}$, $1b_{2u}$, $1b_{2g}$ involve the B 2p and H 1s orbitals. The $3a_g$ is B–B and B–H bonding in both planes. The $1b_{3u}$ is B–B π bonding B–H_t bonding and nonbonding in the bridging plane. The $1b_{2u}$ is B–B π bonding and B–H_b bonding and nonbonding in the terminal plane. The $1b_{2g}$ is B–B antibonding and B–H_t bonding and nonbonding in the bridging plane.

The weakly occupied NO's in Figure 8 are primarily B–H antibonding but contain both B–B bonding, nonbonding, and antibonding interactions. The most important orbitals in terms of their occupation number are the $2b_{3u}$, $1b_{3g}$, $4a_g$, and $3b_{1u}$. The $2b_{3u}$ and $4a_g$ are B–B bonding, π and σ, respectively, while the $1b_{3g}$ and $3b_{1u}$ are B–B antibonding, π and σ, respectively. The next most important orbitals are the $5a_g$ which is B–B σ bonding and the $2b_{2g}$ which is B–B π antibonding. The net effect of electron correlation, which is reflected both in the orbitals and their occupation number, but perhaps more strongly in the electron density, is a decrease in the B–H electron density and an increase in the B–B and B "lone-pair" electron density.

Conclusions. Our results show that the GMO procedure yields a set of primary orbitals which, when used in a CI calculation, account for most of the electron correlation effects on the electron density and on the dissociation energy of diborane. The comparison of the various basis sets shows that polarization functions, including p functions on hydrogen, are necessary for an accurate representation for both the electron density and the dissociation energy. As one improves the basis set, electron density moves into the interior of the cluster, particularly in the bonding regions, while electron correlation moves electron density into previously nonbonding regions, a B–B "bonding" region perpendicular to the bridging plane and the B "lone-pair" region in the bridging plane. Electron correlation affects the bridging hydrogens more than the terminal ones. The decrease in electron density around the bridging hydrogens, when electron correlation is introduced, contributes to their acidic character.

Acknowledgments. This work was supported by the National Science Foundation, Grants CHE 77-07825 and CHE 79-20993.

(20) (a) Mullen, D.; Hellner, E. *Acta Crystallogr., Sect. B* **1977**, *B33*, 3816. (b) Scheringer, C.; Mullen, D.; Hellner, E. *Ibid.* **1978**, *B34*, 621.

(21) Laws, E. A.; Stevens, C. M.; Lipscomb, W. N. *J. Am. Chem. Soc.* **1972**, *94*, 4461.